

Frequency-cycling for compensation of off-resonance effects and improved stability of complex inversions in surface NMR

Denys Grombacher

Stanford University
Stanford, CA, USA
denysg@stanford.edu

Mike Müller-Petke

Liebniz Institute For Applied Geophysics
Hannover, Germany
mike.muller-petke@liag-hannover.de

Rosemary Knight

Stanford University
Stanford, CA, USA
rknight@stanford.edu

SUMMARY

To produce accurate images of subsurface properties using the surface Nuclear Magnetic Resonance (NMR) technique we require accurate modelling of the physics of the excitation process. This demands precise knowledge of the Larmor frequency at all locations in the subsurface. In practice, this is infeasible to achieve. Therefore, we present a method, called frequency-cycling, that ensures an accurate forward model in the presence of an uncertain Larmor frequency estimate. Frequency-cycling reduces sensitivity to the influence of an unknown offset between the estimated and true Larmor frequencies improving the ability of surface NMR to generate images that are representative of the true subsurface. Additionally, frequency-cycling stabilizes the complex inversion of surface NMR data exploiting resolution enhancements associated with complex inversion. We demonstrate the advantages of the frequency-cycling method in both synthetic and field studies.

Key words: surface NMR, off-resonance, magnetic field inhomogeneity, complex inversion

INTRODUCTION

Surface Nuclear Magnetic Resonance (NMR) provides direct sensitivity to water content allowing non-invasive characterization of aquifer properties. The experiment involves measuring the induced voltage in a coil of wire laid on the ground surface following the perturbation of a magnetization present in the subsurface. The magnetization, composed of the sum of nuclear magnetic spin moments of the hydrogen nuclei, is perturbed by pulsing an oscillatory current through a surface coil to generate a secondary magnetic field that induces a torque on the magnetization. Only components of the magnetization transverse to the direction of the background magnetic field (Earth's field) directly contribute to the measured signal.

To produce images of subsurface water content and relaxation times, used to estimate pore-scale properties, the signal is measured after a series of pulsed currents of different pulse moments; the pulse moment is equal to the product of the pulse duration and amplitude. Each pulse moment provides a different spatial sampling of the subsurface properties. The suite of measured signals is then inverted to produce images (depth profiles in 1D) of the subsurface water content and relaxation times. To ensure images representative of the true subsurface are produced we require accurate

modelling of the physics of the perturbation process (called excitation).

The standard surface NMR forward model assumes that the oscillation frequency of the current in the surface coil (transmit frequency, ω_T) is chosen to be equal to the Larmor frequency, ω_0 , of the hydrogen nuclei, called on-resonance excitation. This contains an implicit assumption that ω_0 is spatially invariant and can be determined with a high degree of accuracy. In many situations this condition may not be valid. Magnetic susceptibility contrast leads to ω_0 inhomogeneity (Hurlimann, 1998) and short duration signals lead to poor frequency resolution making accurate determinations of ω_0 difficult. Both of these situations may lead to an estimated Larmor frequency ($\omega_{0,ass}$) distinct from the true Larmor frequency (ω_0). When we intend to induce on-resonance excitation, ω_T is set equal to $\omega_{0,ass}$, which may be distinct from ω_0 in the presence of an unknown offset ($\Delta\omega_{uk}$). This situation is shown in Figure 1a.

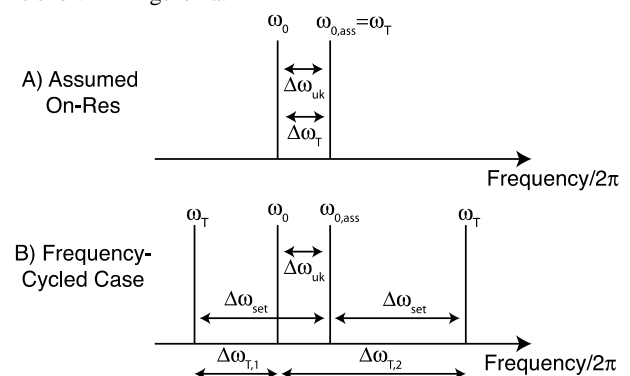


Figure 1. Schematic illustrating the important frequencies when on-resonance excitation is assumed (A), and when frequency-cycling is performed (B) in the presence of an unknown offset between the true and estimated Larmor frequencies.

An offset exists during transmit ($\Delta\omega_T$) between ω_T and ω_0 , in this case equal to $\Delta\omega_{uk}$, causing off-resonance excitation to occur. Off-resonance excitation impacts the signal amplitude, phase, and spatial distribution (Walbrecker et al., 2011a). As such, neglecting off-resonance excitation degrades the accuracy of the forward model potentially reducing the reliability of the surface NMR images. Off-resonance excitation itself does not degrade performance; it simply requires that the forward model be adjusted to properly describe the excitation. However, this is a difficult problem given that we do not always have accurate knowledge of the spatially varying ω_0 and whether $\Delta\omega_{uk}$ is non-zero.

Our proposed solution is to build a method capable of reducing sensitivity to off-resonance effects that arise due to $\Delta\omega_{uk}$ that does not require improved characterization of ω_0 .

We demonstrate that by collecting data at two distinct transmit frequencies, at equal magnitude offsets ($\Delta\omega_{\text{set}}$) above and below $\omega_{0,\text{ass}}$, the data can be stacked in a manner that coherently stacks the signal well described by $\omega_{0,\text{ass}}$ and $\Delta\omega_{\text{set}}$ while destructively combining the portion of the signal due to $\Delta\omega_{\text{uk}}$. As such, it improves the ability of our forward model to accurately describe the excitation process. Figure 1b illustrates schematically this strategy, which we refer to as frequency-cycling, and the relevant frequencies. The concept is similar to phase-cycling, an already implemented technique in surface NMR (Walbrecker et al., 2011b; Grunewald et al., 2014), where the phase of a pulse is alternated to adjust the phase of a particular component of the signal allowing stacking to occur where only a desired component is stacked coherently. We also hypothesize that reduced sensitivity to unknown off-resonance effects associated with $\Delta\omega_{\text{uk}}$ improves the stability of the complex-inversion for surface NMR allowing resolution enhancements associated with the complex-inversion to be exploited. We demonstrate the advantages of frequency-cycling in both synthetic and field studies.

FREQUENCY-CYCLING

The frequency-cycling method aims to exploit a symmetry present in off-resonance excitation. Excitations that occur for offsets of equivalent magnitude but of opposite sign (eg. $+\Delta\omega_{\text{set}}$ and $-\Delta\omega_{\text{set}}$ about ω_0) produce transverse magnetizations with the same y component, and x-components of equivalent magnitude but opposite sign. As such, the signals measured after excitations at offsets of $+\Delta\omega_{\text{set}}$ and $-\Delta\omega_{\text{set}}$ can be stacked to produce the same signal as only the $+\Delta\omega_{\text{set}}$ offset. This is done by adding the real components of each signal (m_y) and taking the difference of the quadrature components (m_x). This allows the stacked signal to be accurately modelled using knowledge of the positive offset only. This is true for the case of $\Delta\omega_{\text{uk}}=0$. The hypothesis we wish to test is whether the ability to describe the frequency-cycled data set using only the positive $\Delta\omega_{\text{set}}$ offset remains true in the presence of non-zero $\Delta\omega_{\text{uk}}$. To test this hypothesis consider Figure 2.

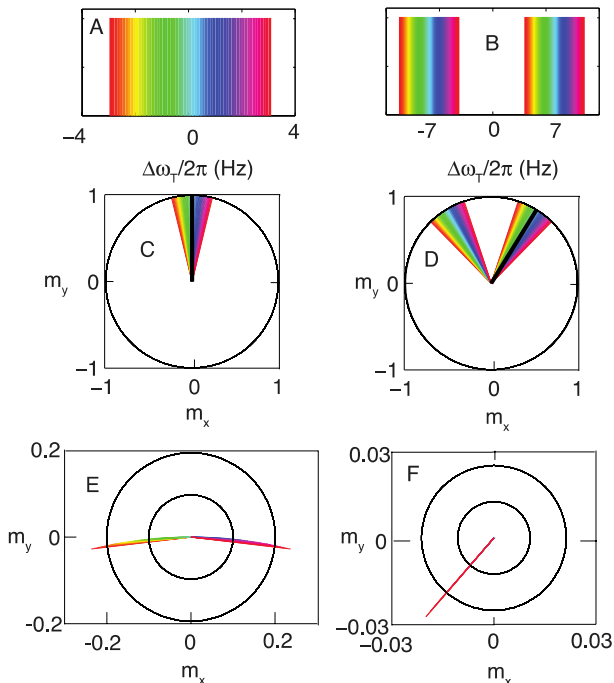


Figure 2. Schematic illustrating the net transverse magnetization following a nominal $\pi/2$ pulse for a 20 ms pulse duration for a $\Delta\omega_{\text{uk}}/2\pi$ range of ± 3 Hz. The left and right columns correspond to the assumed on-resonance and frequency-cycling cases, respectively. A) and B) illustrate the actual offset during transmit ($\Delta\omega_T$), each color corresponds to a different magnitude of $\Delta\omega_{\text{uk}}$. C) and D) illustrate the net transverse magnetization following excitation at each $\Delta\omega_T$. The left and right wedges in D) correspond to the left and right rainbows in B). E) and F) represent the residual, equivalent to the unmodelled component, between the actual transverse magnetizations (colored vectors in C, D) and the modelled transverse magnetization (black vectors in C, D) produced using $\Delta\omega_T/2\pi=0$ and $\Delta\omega_T/2\pi=\Delta\omega_{\text{set}}/2\pi=7$ Hz for the on-resonance and frequency-cycled cases, respectively. The circles in F have radii 10 times smaller than the circles in E. The residual is roughly an order of magnitude smaller in F than in E.

Figure 2 illustrates the difference between the actual transverse magnetization (with $\Delta\omega_{\text{uk}}$ present) and the transverse magnetization predicted by the modelling when we assume either on-resonance or frequency-cycling occurred for a nominal $\pi/2$ 20 ms pulse. We investigate a range of $\Delta\omega_{\text{uk}}$ that varies from -3 Hz (red) to +3 Hz (purple). Figure 2A and 2B illustrate the offsets during transmit for the assumed on-resonance excitations cases ($\Delta\omega_T=\Delta\omega_{\text{uk}}$) and the frequency-cycling cases ($\pm\Delta\omega_T=\Delta\omega_{\text{uk}}\pm\Delta\omega_{\text{set}}$). For the frequency-cycling case $\Delta\omega_{\text{set}}/2\pi=7$ Hz; this value was determined empirically to provide the best performance. Figures 2C and 2D illustrate the actual transverse magnetization after the nominal $\pi/2$ pulse for each $\Delta\omega_T$ (colors). The black lines in Figures 2C and 2D represent the transverse magnetization that would be predicted by the forward model for the on-resonance (i.e. $\Delta\omega_T/2\pi=0$ Hz) and the frequency-cycling cases ($\Delta\omega_T/2\pi=\Delta\omega_{\text{set}}/2\pi=7$ Hz). Note that for the frequency-cycled case, the net transverse magnetization is formed by frequency-cycling each pair of colored vectors (one from each wedge in Figure 2D); done by adding the y components, and subtracting the x-components. Of importance is the ability of our forward model to predict the actual net transverse magnetization in each case. Figure 2E and 2F illustrate the residual between the actual and modelled transverse magnetizations for the on-resonance and frequency-cycled cases, respectively, for each magnitude of $\Delta\omega_{\text{uk}}$. The circles in Figure 2E have radii ten times larger than in Figure 2F. This indicates that the unmodelled component of the transverse magnetization is significantly reduced by frequency-cycling; by roughly an order of magnitude compared to the on-resonance case (Figure 2E). This demonstrates that frequency-cycling has an improved ability to model the net transverse magnetization in the presence of non-zero $\Delta\omega_{\text{uk}}$, equivalent to improving the accuracy of our forward model.

The example in Figure 2 uses a single value of the applied magnetic field. For a surface NMR experiment the applied magnetic field is extremely heterogeneous; to investigate whether the frequency-cycling method still mitigates $\Delta\omega_{\text{uk}}$ in this case consider Figure 3.

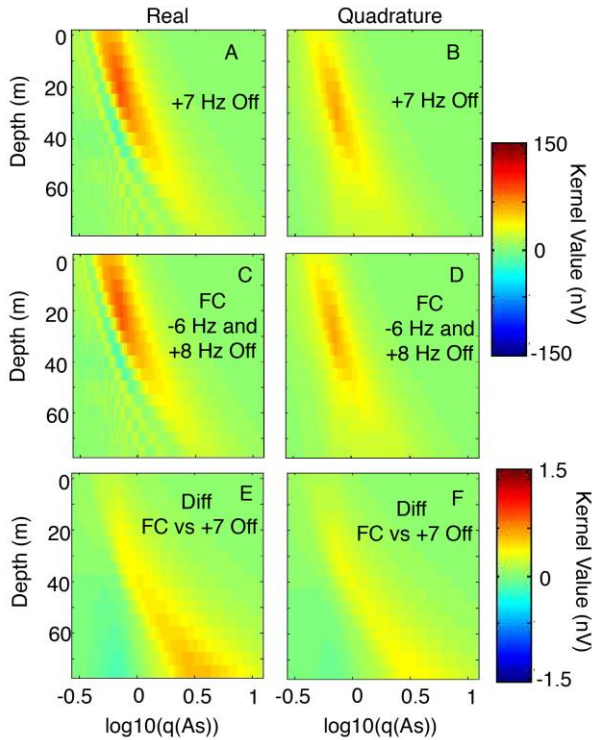


Figure 3. Comparison of the difference between the kernels describing a $\Delta\omega_T/2\pi=+7$ Hz off-resonance excitation (used for the frequency-cycling modelling) (top row) and the kernel describing a frequency-cycled data where $\Delta\omega_{uk}/2\pi=1$ Hz; i.e. excitations actually occurred at $\Delta\omega_T/2\pi=-6$ Hz and $\Delta\omega_T/2\pi=+8$ Hz off-resonance. The bottom row illustrates the difference between the assumed (top row) and actual (middle row) kernels. Note that the color scale in the bottom row is two orders of magnitude smaller than in the top two rows. The left and right columns correspond to the real and quadrature components, respectively. The top two rows use the same colorbar.

In Figure 3 we contrast the kernel we plan to use during the inversion, containing our $\Delta\omega_{set}$ so that $\Delta\omega_T/2\pi=\Delta\omega_{set}/2\pi=7$ Hz, against the kernel that actually describes the frequency-cycled data. In this case, frequency-cycling occurred in the presence of $\Delta\omega_{uk}/2\pi=1$ Hz. This means that although we assumed that excitations took place at $\pm\Delta\omega_T=\pm\Delta\omega_{set}=\pm 7$ Hz during the frequency-cycling, the actual transmit offsets ($\pm\Delta\omega_T=\Delta\omega_{uk}\pm\Delta\omega_{set}$) occurred at -6 Hz and +8 Hz. The middle row of Figure 3 illustrates the kernel describing the frequency-cycled combination of the -6 Hz and +8 Hz offsets. The bottom row illustrates the difference between the kernel to be used in the modelling and the kernel describing the frequency-cycled situation where $\Delta\omega_{uk}/2\pi=1$ Hz. This represents the accuracy of our model in the presence of $\Delta\omega_{uk}/2\pi=1$ Hz. Figure 3E and 3F illustrate that the residual is approximately two orders of magnitude smaller than the actual kernel values, demonstrating that the impact of $\Delta\omega_{uk}$ in this case is minimal. This illustrates that frequency-cycling is expected to mitigate $\Delta\omega_{uk}$ even when the applied magnetic field is heterogeneous.

To demonstrate the reduced sensitivity to unknown offsets Figure 4 illustrates water content estimates for synthetic surveys performed in the presence of varying magnitudes of $\Delta\omega_{uk}$ (colors). The synthetic survey employed a 50 m diameter loop and a 20 ms pulse duration. The subsurface is composed of a halfspace of 75 Ω m and 15%

water content, values representative of realistic subsurface conditions. All data have 10 nV of noise added prior to inversion. The forward model and complex-inversion available within the MRSmatlab software package is employed (Muller-Petke et al., 2012).

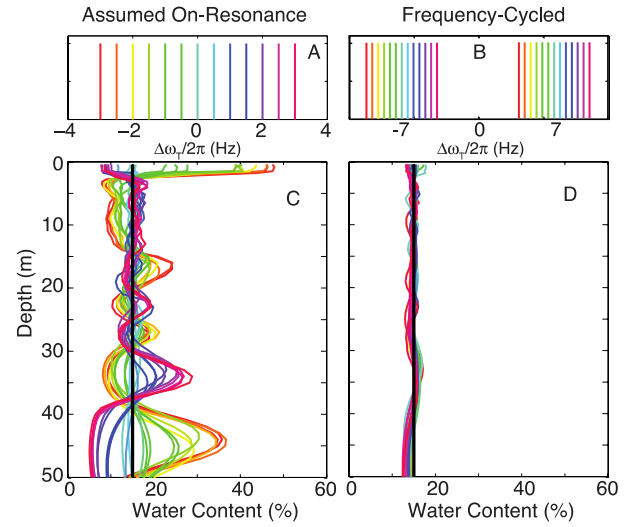


Figure 3. The $\Delta\omega_T$ (top row) for the assumed on-resonance survey ($\Delta\omega_T=\Delta\omega_{uk}$) (A) and the frequency-cycled survey ($\pm\Delta\omega_T=\Delta\omega_{uk}\pm\Delta\omega_{set}$) (B). The water content profiles estimated in the presence of $\Delta\omega_{uk}$ (colors) inverted assuming on-resonance excitation ($\Delta\omega_T=0$) (C) and using a frequency-cycled kernel that assumes $\Delta\omega_T/2\pi = +\Delta\omega_{set}/2\pi = +7$ Hz (D).

Figure 4C illustrates that when on-resonance excitation is assumed in the presence of non-zero $\Delta\omega_{uk}$ the complex-inversion produces poor estimates of the true water content profile (black line). This stems from the kernel not adequately describing the excitation process resulting in the inversion requiring complex structure in the water content profile to fit the observed data. Furthermore, for $\Delta\omega_{uk}/2\pi$ larger than $\sim\pm 3$ Hz the complex-inversion cannot fit the data at all in the on-resonance case, requiring that one resorts to an amplitude inversion. In contrast, the frequency-cycled water content profiles, all produced using the same +7 Hz off-resonance kernel (our assumed $\Delta\omega_T$) during inversion, accurately reproduce the true water content profile for all investigated $\Delta\omega_{uk}$.

To demonstrate the feasibility of the frequency-cycling method in an actual field experiment consider Figure 5, which illustrates the results of a study performed near Schillerslage, Germany. The background magnetic field was observed to vary less than 10 nT (~ 0.4 Hz) during the course of the experiment and $\omega_0/2\pi$ was measured to be 2099 Hz. Excitations were performed at five different values of $\omega_T/2\pi$ [2092 2094 2099 2106 2108] Hz representing $\Delta\omega_T/2\pi$ of [-7 -5 0 7 9] Hz, respectively. This provides an on-resonance survey, and four frequency-cycled pairs. Table 1 describes the combination of the frequency-cycled pairs.

	$\omega_{T1}/2\pi$ (Hz)	$\omega_{T2}/2\pi$ (Hz)	$\omega_{T,inv}/2\pi$ (Hz)	$\Delta\omega_{uk}/2\pi$ (Hz)
FC pair 1	2092	2106	2106	0
FC pair 2	2094	2106	2105	1
FC pair 3	2092	2108	2107	1
FC pair 4	2094	2108	2106	2

Table 1. The frequency-cycled combinations and the corresponding assumed offset (the offset used during inversion). The ω_{T1} and ω_{T2} columns show the transmit frequencies for each frequency-cycled pair, and the $\omega_{T,inv}$ column corresponds to the frequency used during the inversion of the frequency-cycled data. The $\Delta\omega_{uk}/2\pi$ column indicates the corresponding unknown offset that is purposefully neglected in this case.

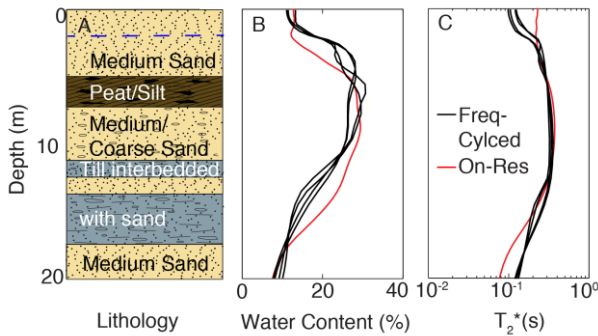


Figure 5. A) Lithology log determined during drilling of a bore-hole at the center of the loop. The estimated water content (B) and T_2^* profiles (C) estimated using the standard on-resonance survey (red) and frequency-cycling methods (black lines).

Both the on-resonance and frequency-cycling methods capture the general features observed in the lithology log, which suggests a trend toward lower water-filled porosity and smaller pore sizes with depth as the sand becomes interbedded with till. We note that the frequency-cycling method detects a T_2^* contrast near the water table (~ 2 m depth). All four frequency-cycling water content and T_2^* profiles closely track one another. The consistency of each estimate, despite the fact that the estimates are formed by data sets collected at four different frequencies, combined in four different manners, and inverted with three different kernels, while purposefully ignoring non-zero $\Delta\omega_{uk}$ for three of the cases, demonstrates the reliability of the frequency-cycling method.

RESULTS AND DISCUSSION

The frequency-cycling method provides an improved ability of the forward model to accurately describe the physics of the excitation process. The frequency-cycling method does not require a new forward model, but rather presents a data acquisition and processing strategy that allows our forward model to better describe the excitation in the presence of an uncertain Larmor frequency estimate. Furthermore, it alleviates the influence of a spatially varying $\Delta\omega_{uk}$, such as one due to a regional magnetic field gradient. For a 20 ms pulse duration the frequency-cycling method is observed to mitigate $\Delta\omega_{uk}/2\pi$ in the range of ± 3 Hz. Shorter and longer pulses used during frequency cycling mitigate larger and smaller $\Delta\omega_{uk}$ ranges, respectively.

An additional advantage of the frequency-cycling method is that it allows broader implementation of the complex-inversion. By reducing the impact of $\Delta\omega_{uk}$, which leads to challenges describing the signal phase, the improved resolution offered by complex-inversion (Braun et al., 2005) can be exploited.

Note that the frequency-cycling method is intended for use with free-induction decay measurements only. Multi-

pulse methods remain better suited to standard on-resonance pulses.

CONCLUSIONS

A method is presented to alleviate the influence of an unknown offset between the true and estimated Larmor frequency, thus improving the accuracy of the surface NMR forward model. By transmitting at two distinct frequencies, at equal magnitude offsets above and below the estimated Larmor frequency, the data can be stacked in a manner that allows the component of the signal due to an unknown offset to be significantly reduced. Frequency-cycling also allows the complex inversion to be more widely implemented by stabilizing the inversion with a more accurate forward model.

The combination of off-resonance excitation and complex-inversion allows the advantages of both to be exploited producing images with improved resolution that are accurate representations of the true subsurface. As such, any method that uses surface NMR as a tool for subsurface characterization stands to benefit from frequency-cycling.

ACKNOWLEDGMENTS

Denys Grombacher was supported by funding from the Stanford School of Earth Sciences and the Conoco Phillips Fellowship. We would also like to acknowledge the use of the MRSmatlab software package.

REFERENCES

- Braun, M., Hertrich, M., and Yaramanci, U., 2005, Study on complex inversion of magnetic resonance sounding signals, *Near Surface Geophysics*, 3, 155-163.
- Grunewald, E., Knight, R., and Walsh, D., 2014, Advancement and validation of surface nuclear magnetic resonance spin-echo measurements of T_2 , *Geophysics*, 79 (2), EN15-EN23.
- Hürlimann, M.D., 1998, Effective gradients in porous media due to susceptibility contrast, *Journal of Magnetic Resonance*, 131 (2), 232-240.
- Müller-Petke, M., Walbrecker, J.O., Costabel, S., Günther, T., and Hertrich, M., 2012, MRSmatlab – A toolbox for modeling, processing, and inverting surface-NMR data, magnetic resonance in the subsurface: Presented at the 5th international workshop of magnetic resonance.
- Walbrecker, J.O., Hertrich, M., and Green, A.G., 2011a, Off-resonance effects in surface nuclear magnetic resonance: *Geophysics*, 76 (2), G1-G12.
- Walbrecker, J.O., Hertrich, M., Lehmann-Horn, J.A., and Green, A.G., 2011b, Estimating the longitudinal relaxation time T_1 in surface NMR: *Geophysics*, 76 (2), F111-F122.